Ab Initio Modeling of Proton Transfer in Phosphoric Acid Clusters

Linas Vilciauskas,[†] Stephen J. Paddison,*[,‡] and Klaus-Dieter Kreuer[†]

Max-Planck-Institut für Festkörperforschung, Heisenbergstrasse 1, D-70569 Stuttgart, Germany, and Department of Chemical and Biomolecular Engineering, University of Tennessee, Knoxville, Tennessee, 37996

Received: April 1, 2009; Revised Manuscript Received: May 9, 2009

Development of superior electrolytes for fuel cells that enable operation at temperatures above 120 °C without external humidification will benefit from molecular-level understanding of proton conduction mechanisms in neat acid systems possessing little or no water. The energetics and collective molecular effects associated with proton transfer in clusters consisting of two to six phosphoric acid (H_3PO_4) molecules are examined with electronic structure calculations. Global minimum-energy structures are determined at the B3LYP/6-311G** level for each cluster from many chemically rational initial configurations. Binding energies are computed and found to correlate with the number and type of hydrogen bonds present in the cluster and show an increase in the strength of the interactions up to and including $(H_3PO_4)_6$. This suggests that more than six molecules may be required to fully encompass the binding in bulk phosphoric acid. Potential energy profiles and associated energetic penalties for proton transfer are determined at the B3LYP/6-31G** level under four different constraints on the positions of surrounding atoms. The endothermicities decrease with increasing cluster size, suggesting that several molecules facilitate proton transfer. Calculation of partial atomic charges with the CHELPG scheme both prior to and following proton transfer indicates a higher degree of charge delocalization in the larger clusters and thereby a smaller energetic penalty.

I. Introduction

Proton transfer is of vital importance in many chemical and biological systems and processes.[1] The conduction of protons plays a central role in the function of many devices, including polymer electrolyte membrane (PEM) fuel cells.[2] Recently, the ability of fuel cells to generate electric power with no greenhouse gas emissions and at high efficiency has generated tremendous interest from various research and industrial communities. The search for novel high-performance electrolytes suitable for low- and intermediate-temperature operation where no external humidification is required has spurred efforts including synthesis and characterization of a wide range of materials suitable as the separator. The development of new materials requires a fundamental understanding of the proton-conduction process at the atomic level, and an Edisonian approach for synthesizing new membrane materials is insufficient.[3]

Proton transfer involves bond-breaking and -forming processes and the transfer of H^+ between two entities accompanied by a local redistribution of electron density.[4] Despite the diversity of proton-conducting electrolyte materials,[5,6] the protonic defects in these materials are solvated by very few species,[7] water, oxide ions, heterocycles, and oxo acids and anions. These species are typically responsible for the intrinsic generation of charge carriers, but a molecular description of the mechanism of proton transfer has only been secured for an excess proton in water.[8] A complete understanding of the solvation structure and dynamics of an excess proton in water, however, remains elusive.[9] It is widely recognized that hydrogen bonding is a key feature in all systems exhibiting proton transport. Of relevance for understanding proton conduction in PEMs is the consideration of ingredients that encompass complexity, connectivity, and cooperativity.[10,11] Investigation of hydrogen bonding from structural as well as dynamical aspects is warranted in order to understand the phenomena at a molecular level. There are few experimental techniques capable of probing the effects accompanying the hydrogen-bond formation or breaking at this scale, and therefore, various simulation methods have been utilized for describing these processes.

Proton mobility in liquid water surpasses the hydrodynamic limit by a factor of more than 4.5 and is approximately five times higher than that of Li^+ in water.[12] The first hypothesis in trying to explain this behavior comes with a picture of highly correlated charge-transfer events along the hydrogen-bonded chains, also known as structure diffusion or Grotthuss hopping.[13] However, a process involving only proton-transfer events between water molecules along the chains leads to a local polarization of the network and no net conduction. Thus, a successive reorientation of the molecules in the outer hydration shell is necessary in order to depolarize the network and yield a new configuration permitting the next proton-transfer event. The first mechanistic picture for the overall excess proton-transfer mechanism in water was determined from NMR data interpreted by Agmon[4] and confirmed by Tuckerman et al.[14,15] with Car−Parrinello ab initio molecular dynamics (AIMD) simulations.[16] The region containing the excess proton corresponds to either a hydrated hydronium ion (i.e., $H_9O_4^+$ or Eigen cation[17,18]) or a dimeric form sharing the excess charge between two water molecules (i.e., a $H_5O_2^+$ or Zundel cation[19]). The proton-transfer mechanism in water proceeds via a series of structural rearrangements between these patterns; in this manner, an Eigen ion is transformed into a Zundel ion, which itself is converted to an Eigen ion (i.e., EZE mechanism[8]). The main qualitative features complemented with some significant quantitative corrections of the above-described mechanism were later

* To whom correspondence should be addressed. E-mail: spaddison@utk.edu.
[†] Max-Planck-Institut für Festkörperforschung.
[‡] University of Tennessee.

10.1021/jp903005r CCC: $40.75

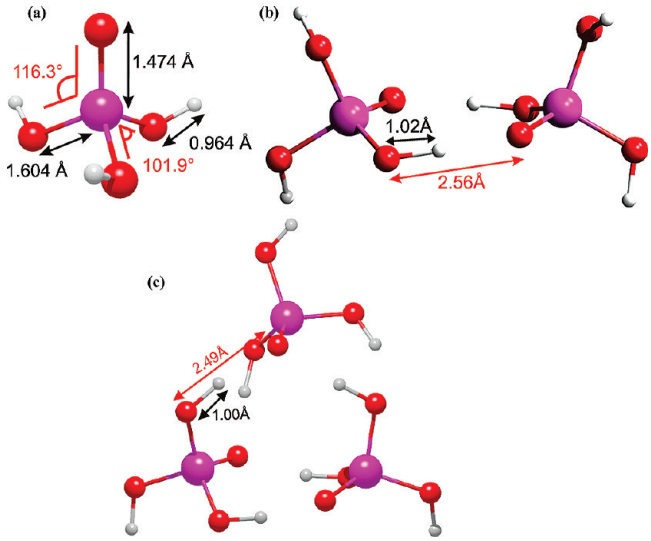

Figure 1. Global minimum-energy structures of phosphoric acid clusters determined at the B3LYP/6-311G** level; (a) H_3PO_4, (b) $(H_3PO_4)_2$, and (c) $(H_3PO_4)_3$.

confirmed by more sophisticated techniques involving nuclear quantum effects.[20−24]

The structure of neat liquid phosphoric acid (H_3PO_4) consists of an extended intermolecular network of hydrogen bonds and exhibits high proton conductivity, making it of particular interest for use in fuel cells. Phosphoric acid fuel cells (PAFCs), in contrast to PEM fuel cells, use phosphoric acid (instead of a solid polymer) as the electrolyte, do not require water for operation, and operate at higher temperature (150−200 °C). Although PAFCs dominate the stationary fuel cell market, there are some serious drawbacks due to low efficiency and a much lower power to size ratio when compared to those for other fuel cells.[25]

Recently, phosphoric acid has become an important constituent of alternative proton-conducting membranes, particularly in complexes with basic polymers, such as poly(benzimidazole) for use as the electrolyte in PEM and direct methanol fuel cells.[26] Despite the fact that the PBI/PA composite has a very low conductivity (~2×10^{-3} S/cm), it has extraordinary thermomechanical and chemical stabilities, which are crucial for fuel cell applications.[27,28] Drawbacks in these systems indicate the fact that H_3PO_4 is not strongly bound to the polymer and therefore leaches out by water during fuel cell operation and also that the proton conductivity dramatically decreases with decreasing concentration of PA. The latter is a common feature in both phosphoric and phosphonic acid systems.[29] Obviously, proton conduction in phosphoric acid is very sensitive toward perturbations, but it is not clear to what extent these perturbations are the consequences of chemical interaction or just the confinement in the diverse matrixes. Of course, such questions can only be addressed in a meaningful way on the basis of a better understanding of proton dynamics in pure bulk phosphoric acid.

The H_3PO_4 molecule has three proton-donor sites and one proton-acceptor site. As a liquid, it is able not only to solvate the excess charge but also generate the charge carriers through self-dissociation (~7.4%) along with some condensation, mainly yielding pyrophosphoric acid ($H_4P_2O_7$).[30] The acid has a low diffusion coefficient of phosphate "blocks" but an extremely high proton mobility, which presumably proceeds via proton transfer between phosphate species and is facilitated by structural rearrangement. The contribution of Grotthuss-type hopping is ~98%, with the remaining 2% coming from hydrodynamic diffusion of charged species.[31,32] Greenwood and Thompson[33,34] were the first to suggest a mechanism for proton conduction in phosphoric acid by introducing Grotthuss chains and a mechanism where the proton hops between neighboring phosphate species. The observation of almost negligible changes in the mobility with an exchange of H with D suggests that the transfer of the proton between phosphate units occurs with very small barriers, and quantum effects might be excluded from the description of the structural mechanism. Most of the previous simulation work aimed at modeling the structure of liquid and solid states was performed using empirical interatomic potentials, which are unable to describe bond-breaking and -forming processes in such a complex system as phosphoric acid.[35] A more recent AIMD study[36] was unable to provide insight into the mechanism of proton transfer in this system in part due to the short time of the simulations.

The aim of this study is to investigate the hydrogen-bonding and proton-transfer energetics in phosphoric acid clusters with ab initio electronic structure calculations. Clusters of up to six molecules are investigated using density functional theory and a moderate size basis set in order to probe collective effects on the proton-transfer potentials and the critical number of molecules necessary for an effective proton-transfer event. Previous studies of similar scope and employing the same computational protocol performed on phosphonic acid, sulfonic acid, and imidazole systems have proved to yield results which were in good agreement with experimental data.[37] The paper is organized as follows; the first section contains a short description of the computational methods used to determine the structures and energetics for all molecular systems. This methods section is followed by a discussion section describing the structures and binding energies for each of the phosphoric acid clusters.

II. Computational Methods

All ab initio self-consistent field (SCF) electronic structure calculations were performed using the GAUSSIAN 03 suite of programs.[38] Geometry optimizations were undertaken by con-

TABLE 1: Energetics of Phosphoric Acid Clusters[a]

	E_{elec}[b]	E_{elec} + ZPE[c]	ΔE_{ZPE}[d] (kcal/mol)	ΔE_{BSSE}[e] (kcal/mol)	ΔE[f] (kcal/mol)
H_3PO_4	−644.26915543	−644.220472			
$(H_3PO_4)_2$	−1288.57984231	−1288.480654	24.9	20.6	10.3
$(H_3PO_4)_3$	−1932.89566541	−1932.743450	51.5	38.9	13.0
$(H_3PO_4)_4$	−2577.20464982	−2577.001550	75.1	57.6	14.4
$(H_3PO_4)_5$	−3221.50301674	−3221.248376	91.6	68.5	13.7
$(H_3PO_4)_6$	−3865.82725131	−3865.524367	126.5	99.0	16.5

[a] All structures optimized at the B3LYP/6-311G** level. [b] Total electronic energy in Hartrees. [c] Total electronic energy corrected for zero point energy (ZPE). [d] Energy difference based on ZPE-corrected E_{elec}. [e] BSSE- and ZPE-corrected binding energy. [f] Binding energy per phosphoric acid molecule.

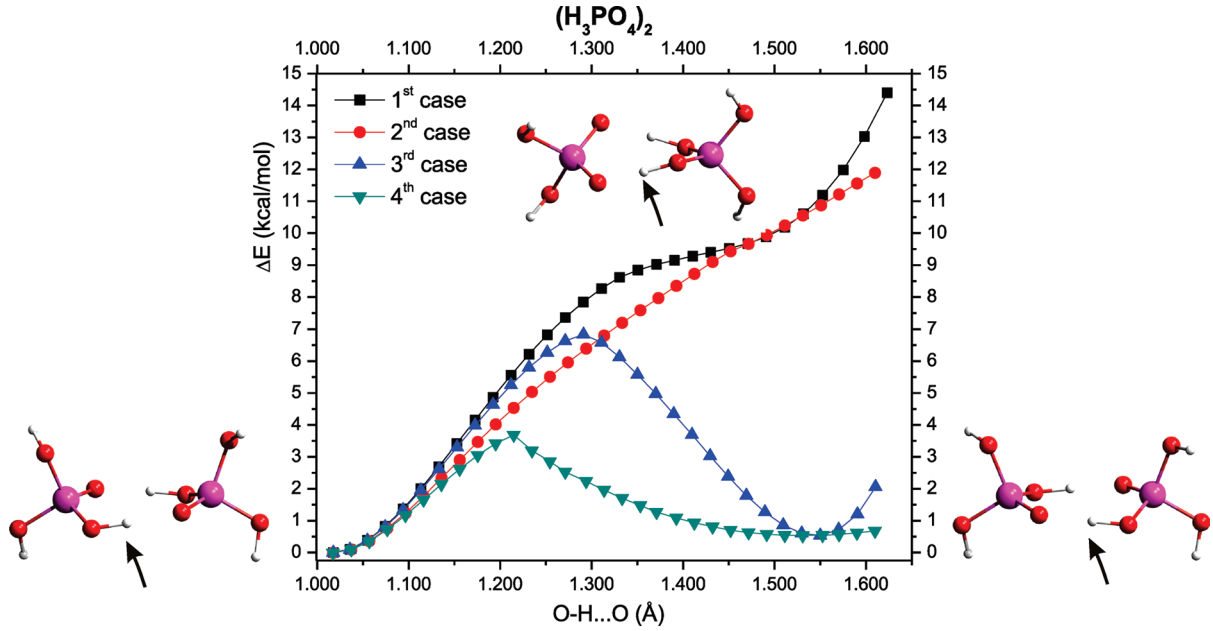

Figure 2. Energetics for proton transfer in $(H_3PO_4)_2$; first case, constraint of the O···O distance of the hydrogen bond where the proton is transferred and the O−H bond length of the second (i.e., back) hydrogen bond; second case, constraint on the O−H bond length only; third case, constraint of the O···O distance only; and fourth case, no constraints. The different configurations shown correspond to the fully optimized dimer (left), the structure following proton transfer under the first constraint (top), and the structure resulting from proton transfer without any constraint, the forth case (right).

jugate gradient methods[39] without symmetry constraints, initially using Hartree−Fock theory with the 6-31G** split valence basis set.[40] The resulting structures were further refined with density functional theory (DFT) and Becke's three-parameter functional (B3LYP),[41−43] first with the same basis set and then with the larger 6-311G**. This procedure was found to be the most efficient in obtaining the global minimum-energy structure at the B3LYP/6-311G** level. The effects of diffuse functions on the minimum-energy configurations were assessed, but only minor differences in the structural parameters with a systematic difference in the total energy were observed. The binding strength (due to hydrogen bonding) was evaluated at the B3LYP/6-311G** level and subsequently corrected for zero-point energy (ZPE) and basis set superposition error (BSSE), the latter using the counterpoise correction (CP) scheme of Boys and Bernardi,[44] which has been known to change the location of local minima in some systems.[45] The energy barrier for proton transfer between phosphoric acid molecules was determined using the potential energy surface (PES) scan method as implemented in GAUSSIAN 03. A hydrogen atom was transferred between phosphate species with an incremental distance of 0.02 Å, and the transition structure at each point of the scan was optimized at the B3LYP/6-31G** level under different constraints to neighboring oxygen atoms and O−H bond distances. Partial atomic electrostatic charges were computed with the CHELPG scheme due to its small dependence on basis set size.[46] The influence of collective effects on the proton-conduction mechanism was probed by examining different clusters consisting of two to six H_3PO_4 molecules.

III. Results and Discussion

H_3PO_4 Molecule. The minimum-energy structure of a single phosphoric acid molecule was determined at the B3LYP/6-311G** level using the methodology described above and is shown in Figure 1a along with important structural parameters including bond lengths and angles. The corresponding energetics are given in Table 1, facilitating the calculation of binding energies in the H_3PO_4 clusters described below.

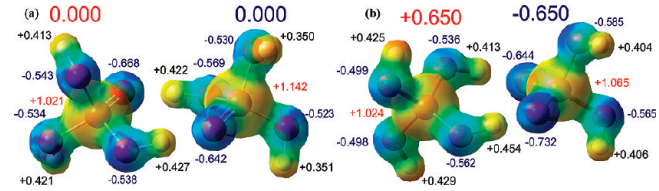

Figure 3. Partial atomic (CHELPG) charges and the electrostatic isosurface for $(H_3PO_4)_2$, (a) prior to proton transfer and (b) following proton transfer under the constraint of back transfer of the second proton (i.e., the first case in Figure 2).

$(H_3PO_4)_2$. A pair of H_3PO_4 molecules were arranged in various conformations with respect to hydrogen-bonding and "twist" angles and fully optimized using the above-described procedure. The global minimum-energy conformation (confirmed through a vibrational frequency analysis) is shown in Figure 1b and has a regular dimeric structure with the molecules bound with a pair of typical hydrogen bonds. As expected, there is a slight increase in the O−H bond distance (1.02 Å) for the protons involved in the hydrogen bonds. The electronic energies are reported in Table 1, and after correcting for ZPE and BSSE, the binding energy was calculated to be 20.6 kcal/mol (10.3 kcal/mol per H_3PO_4).

PES scans along the proton-transfer coordinates with respect to four different constraints on neighboring oxygen atoms and O−H bonds in the pair of phosphoric acid molecules were performed, and the profiles for each of the cases are shown in Figure 2. The first case corresponds to the situation where the oxygen−oxygen separation distance of the hydrogen bond where the proton is transferred is fixed and the O−H bond length in the second hydrogen bond is held constant. In the second case, the constraint on the O−H bond length is retained, but the restriction on the O···O distance is relaxed. The final two cases represent situations of decreasing constraint, where, in the third case, only the O···O distance for the hydrogen bond considered is fixed, and no constraints are imposed in the fourth case. The last two cases represent the situation where the O−H

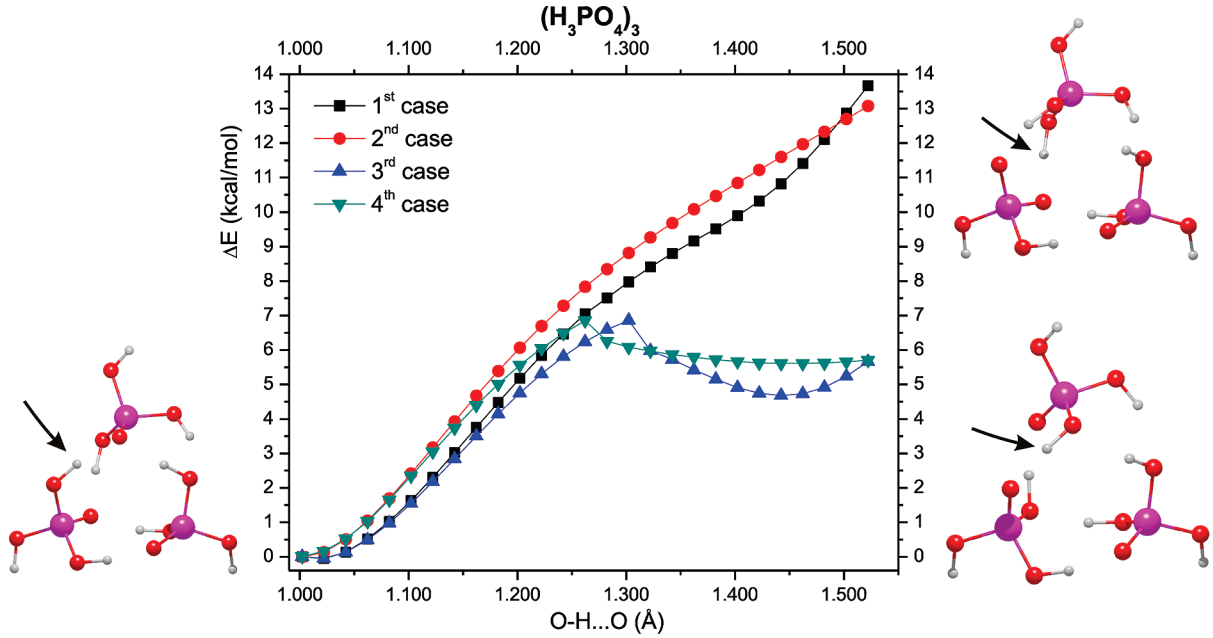

Figure 4. Energetics for proton transfer in $(H_3PO_4)_3$ with the position of the transferred proton indicated by an arrow in each of the three configurations. First case, constraint of the O···O distance of the hydrogen bond where the proton is transferred and the O−H bond length of the neighboring hydrogen bond; second case, constraint on the O−H bond length only; third case, constraint of the O···O distance of the hydrogen bond where the proton is transferred only; and fourth case, no constraints. The different configurations shown correspond to the fully optimized dimer (left), the structure following proton transfer under the first constraint (top right), and the structure resulting from proton transfer without any constraint, the fourth case (bottom right).

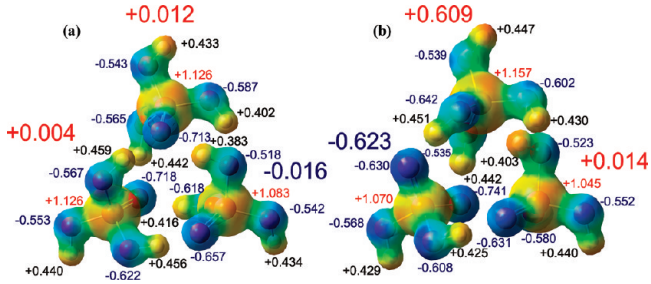

Figure 5. Partial atomic charges and electrostatic isosurface for $(H_3PO_4)_3$ (a) before and (b) following proton transfer under the constraint of back transfer of the second proton (i.e., first case in Figure 4).

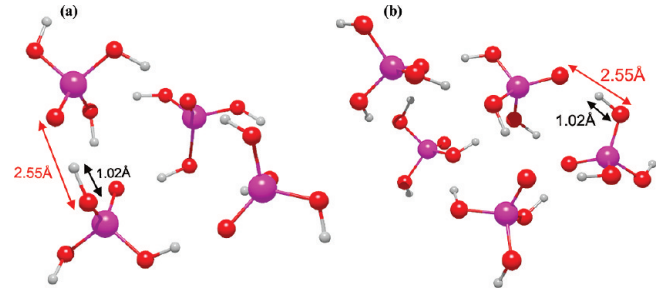

Figure 6. Fully optimized structures of phosphoric acid clusters determined at the B3LYP/6-311G** level; (a) $(H_3PO_4)_4$ and (b) $(H_3PO_4)_5$.

bond length of the second hydrogen bond is not fixed, and hence, charge separation is not forced with the transfer of the proton. The more relaxed optimizations as indicated in Figure 2 result in lower energetic barriers (6.8 and 3.7 kcal/mol for cases three and four, respectively) and fairly symmetric energy profiles with respect to the center of the hydrogen bond, demonstrating that with the "back" transfer of the other proton in the second hydrogen bond, the final configuration strongly resembles the starting configuration with only a slightly higher (∼0.5 kcal/mol) energy and very minor changes in the positions of the atoms (left and right configurations in Figure 2). The endothermicity associated with protonating an acid and the consequent formation of the $[H_4PO_4^+][H_2PO_4^-]$ ion pair was calculated to be 11.2 kcal/mol. This is significantly higher than that for the cases where no charge separation results from proton transfer (i.e., 0.5 kcal/mol for cases three and four). Analysis of the partial (CHELPG) atomic charges for both the global minimum-energy structure and the resulting configuration where back transfer of a second proton was prohibited (i.e., cases one or two) indicates that proton transfer results in a net charge transfer of 0.650 (Figure 3), with most of it coming from the charge redistribution on the oxygen atoms involved in the two hydrogen bonds.

$(H_3PO_4)_3$. A number of distinct input geometries were selected for constructing molecular clusters consisting of three phosphoric acid molecules and optimized following the scheme described previously for the dimer. However, in this case, several distinctly different local minimum-energy structure configurations were obtained. The "global" minimum-energy structure, shown in Figure 1c, was selected as the configuration with the lowest energy among the different isomeric clusters and indicates that several degrees of freedom exist in the configuration space of this relatively small system consisting of only three molecules. The minimum-energy cluster has six hydrogen bonds with O···O separation distances ranging from 2.49 up to 2.70 Å. The BSSE-corrected binding energy (see Table 1) for the phosphoric acid trimer is 38.9 kcal/mol, resulting in 13.0 kcal/mol per H_3PO_4 molecule. This value is significantly higher than that computed for the dimer and is probably due to the fact that the trimer has three hydrogen bonds of moderate length [d(O−H···O) = ∼2.6 Å], one significantly longer "quasi-hydrogen bond" [d(O−H···OH = ∼2.7 Å)], and a much shorter hydrogen bond in which the proton is transferred [d(O−H···O) = ∼2.5 Å]. The computed energetics for transfer of a proton under each of the constraints is shown in Figure 4, with the position of the selected proton indicated with an arrow

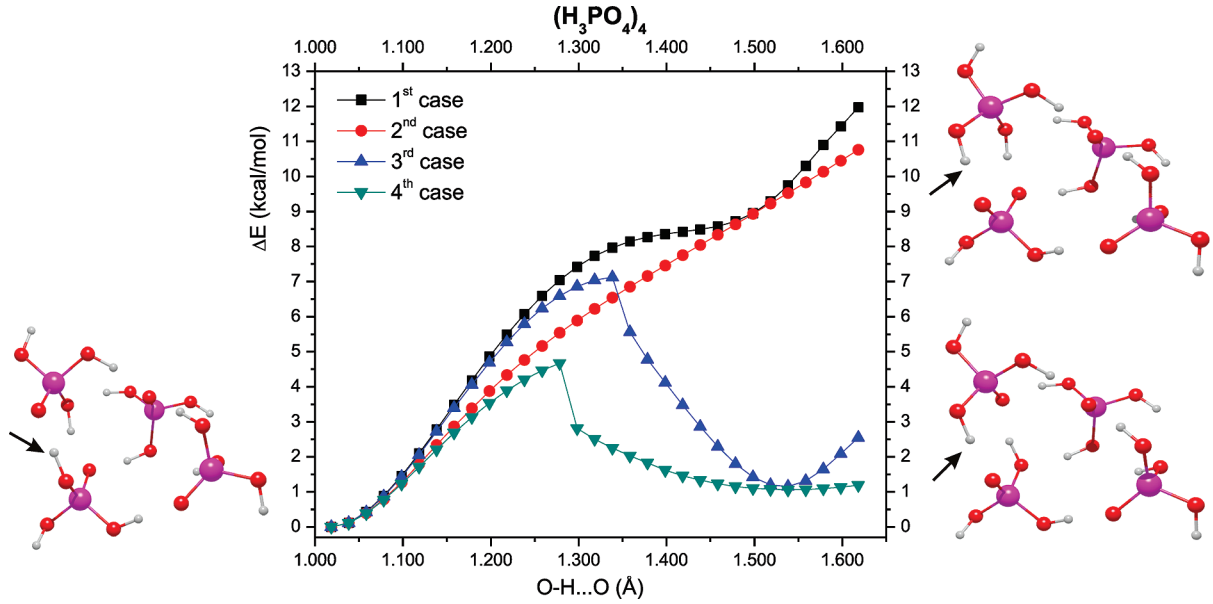

Figure 7. Energetics for proton transfer in $(H_3PO_4)_4$; first case, constraint of the O···O distance of the hydrogen bond where the proton is transferred and the O−H bond length of the neighboring hydrogen bond; second case, constraint on the O−H bond length only; third case, constraint of the O···O distance of the hydrogen bond where the proton is transferred only; and fourth case, no constraints. The different configurations shown correspond to the fully optimized dimer (left), the structure following proton transfer under the first constraint (top right), and the structure resulting from proton transfer without any constraint, the fourth case (bottom right).

in each of the three configurations. The penalty for moving the proton under constraint that results in the formation of $[H_4PO_4^+][H_3PO_4^-][H_3PO_4]$ (see the configuration at the top right in Figure 4) is 10.8 kcal/mol, which is ∼0.5 kcal/mol lower than that in the dimer (Figure 2). It is important to point out that calculation of partial atomic charges indicates a slight redistribution of charges (approximately ±0.01) (Figure 5a) even before transferring the proton between the phosphates. The transfer of the proton, as expected, substantially increases the negative charge on the donating molecule (i.e., a decrease of 0.627) and demonstrates not only an increase in the positive charge of the protonated molecule but also one on the third H_3PO_4 in the cluster, the latter by 0.030. The magnitude of charge transferred is slightly less than that observed in the dimer (−0.650) through the delocalization of positive excess charge in the cluster. The respective decrease in the energetic penalty for shuttling the proton and separating the charge, as well as a higher degree of charge delocalization, suggest that all of the molecules comprising the cluster participate in the intermolecular proton-transfer process of this system.

$(H_3PO_4)_4$. The investigation was extended to clusters consisting of four phosphoric acid molecules in order to check the trends observed for the two and three molecular clusters. Clusters of four H_3PO_4 molecules in various configurations were constructed, including a configuration corresponding to the bonding exhibited by the crystalline state of phosphoric acid, determined by neutron diffraction.[47,48] The configuration taken from the solid, as expected, exhibits the strongest interaction between the acid molecules and hence the lowest electronic energy. After optimization at the B3LYP/6-311G** level, some slight changes in the atomic positions as well as an increase in the irregularity of the hydrogen bonding was observed, and the resulting configuration is shown in Figure 6a. However, an interesting effect was observed during the PES scans of some of the configurations, namely, that with fewer constraints during the proton transfer, clusters undergo structural rearrangements, yielding new more stable geometries. This information was further used for locating the global minimum. Moreover, a

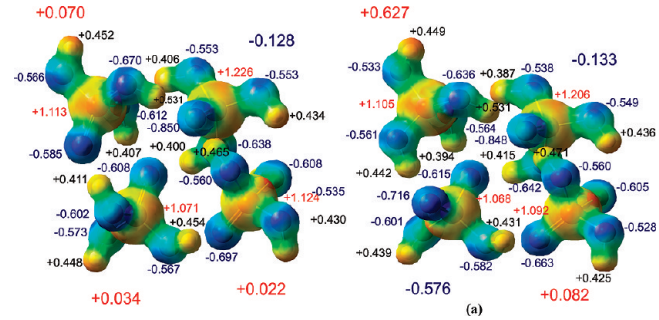

Figure 8. Partial atomic charges and electrostatic isosurface for the $(H_3PO_4)_4$ (a) before and (b) following proton transfer under the constraint of back transfer of the second proton (i.e., first case in Figure 7).

number of interesting features were observed during the geometry reoptimizations, such as greater irregularity of hydrogen bonding and consequential greater distribution in the length of the hydrogen bonds. The binding energy, after correction for ZPE and BSSE, was calculated to be 57.6 kcal/mol for the entire cluster, giving 14.4 kcal/mol/H_3PO_4, 1.3 kcal/mol higher than that observed with the trimer. The energetic penalty for transferring the selected proton from one H_3PO_4 molecule to another was determined to be about 9.6 kcal/mol under conditions where both the O···O distance and O−H bond length are constrained, shown in Figure 7 (top right configuration). Relaxing the atoms surrounding the hydrogen bond over which the proton is transferred significantly reduces the endothermicity and the activation barrier, as revealed in the third and fourth cases in Figure 7. The energetic comparison between the lowest-energy trimeric and tetrameric configurations confirms the trends of easier charge separation and a lower activation barrier for proton transfer in a larger system. The extent to which charges are partitioned in the system and the resulting dipolar moment induced were also evaluated. The computed partial atomic charges of the global minimum-energy structure and the configuration exhibiting charge separation (i.e., $[H_3PO_4]_2[H_4PO_4^+][H_3PO_4^-]$, case one) are shown in Figure 8a and b,

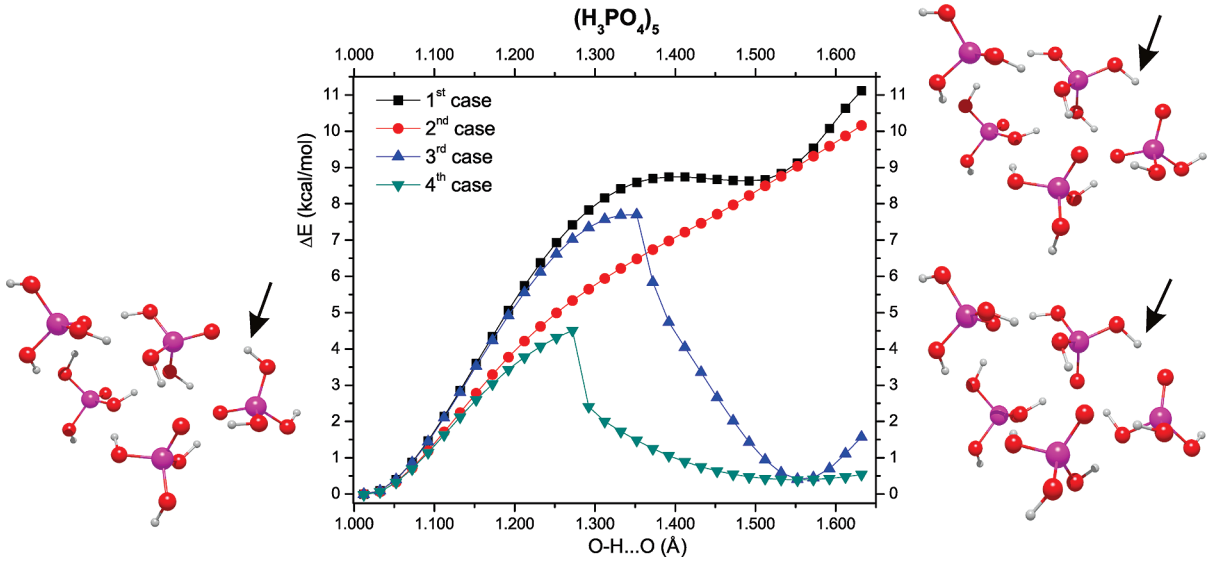

Figure 9. Energetics for proton transfer in $(H_3PO_4)_5$; first case, constraint of the O···O distance of the hydrogen bond where the proton is transferred and the O−H bond length of the neighboring hydrogen bond; second case, constraint on the O−H bond length only; third case, constraint of the O···O distance of the hydrogen bond where the proton is transferred only; and fourth case, no constraints. The different configurations shown correspond to the fully optimized dimer (left), the structure following proton transfer under the first constraint (top right), and the structure resulting from proton transfer without any constraint, the fourth case (bottom right).

respectively. The atomic charges on the molecules after the proton transfer were slightly lower in magnitude than those observed in either the dimer or trimer. The estimated total charges on the conjugate acid and conjugate base were +0.627 and −0.576, respectively, with the rest of the negative charge delocalized on the neighboring phosphoric acid molecules.

$(H_3PO_4)_5$. Starting configurations for a cluster consisting of five phosphoric acid molecules were selected from geometries observed in the crystalline arrangement. The resulting global minimum-energy configuration obtained at the B3LYP/6-311G** level is presented in Figure 6b. The configuration clearly reveals an increase in the distribution in the lengths and types (i.e., O−H···O and O−H···OH) of the hydrogen bonds. The structure has nine hydrogen bonds of moderate length and two extended hydrogen bonds. The binding energy for this cluster after correction for ZPE and BSSE is 69.8 or 14.0 kcal/mol/H_3PO_4. This binding energy per phosphoric acid molecule is similar to that computed in the cluster consisting of four molecules and is undoubtedly due to the similarity in the number of conventional hydrogen bonds in each of the clusters (seven and nine for the $(H_3PO_4)_4$ and $(H_3PO_4)_5$ clusters, respectively). The energy profiles for proton transfer under the four different constraints are shown in Figure 9. The energy penalty for proton transfer under full constraint on the coordinates of surrounding atoms is ∼8.9 kcal/mol. With relaxation of the neighboring O−H bond, the barrier height is substantially reduced (∼4.5 kcal/mol), and the energy difference between the initial and final states is almost negligible. This indicates an almost pure double proton migration inside of the complex without any structural rearrangements or charge redistribution (compare the configuration on the left with the lower figure on the right in Figure 9). The top of the potential barrier shifts closer to one of the oxygen atoms, thus revealing some contraction of the hydrogen bond and the effect of a second oxygen atom, facilitating the proton transfer. The charge analysis is shown in Figure 10 and reveals that the charges resulting due to the proton transfer are of the same order as those in the case of previous clusters, conjugate acid (−0.669) and conjugate base (+0.562). However, a significant part of an excess positive charge (+0.169) is located on two neighboring molecules, suggesting that more molecules

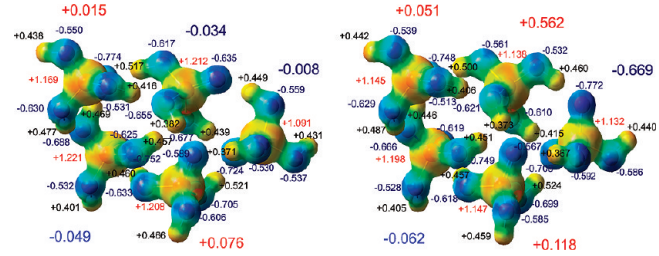

Figure 10. Partial atomic charges and electrostatic isosurface for $(H_3PO_4)_5$ (a) before and (b) following proton transfer under the constraint of back transfer of the second proton (i.e., first case in Figure 9).

in the system facilitate the overall charge delocalization and might be a reason for the decreasing charge separation energy with an increasing system size.

$(H_3PO_4)_6$. The final stage of this study was the investigation of proton-transfer energetics in a cluster consisting of six phosphoric acid molecules. The starting coordinates were again taken from the solid-state arrangement, and the global minimum-energy configuration optimized at the B3LYP/6-311G** level is shown in Figure 11. The ZPE- and BSSE-corrected binding energy per phosphoric acid molecule in the cluster is 16.5 kcal/mol. This is a significant increase over the binding energies computed for the clusters with four and five molecules and suggests that larger clusters are probably needed to obtain the binding energies approaching that in the extended (i.e., bulk) system. PES scans were performed under the same four levels of constraint for proton transfer over one of the short hydrogen bonds, and the corresponding potential energy profiles are plotted in Figure 12. Clearly, the energy profiles have become essentially flat, with all barriers less than 1.2 kcal/mol. This may be due to the very short hydrogen bond [d(O···H) = 1.42 Å] over which the proton transfer occurs; however, an almost identically short hydrogen bond [d(O···H) = 1.47 Å] in a trimeric cluster resulted in a significantly higher PT barrier. With an analogy to all other systems, the CHELPG analysis of partial charges on atoms was performed. The results are presented in Figure 13. As one might expect, the charge delocalization is higher in this system even prior to proton transfer (see Figure

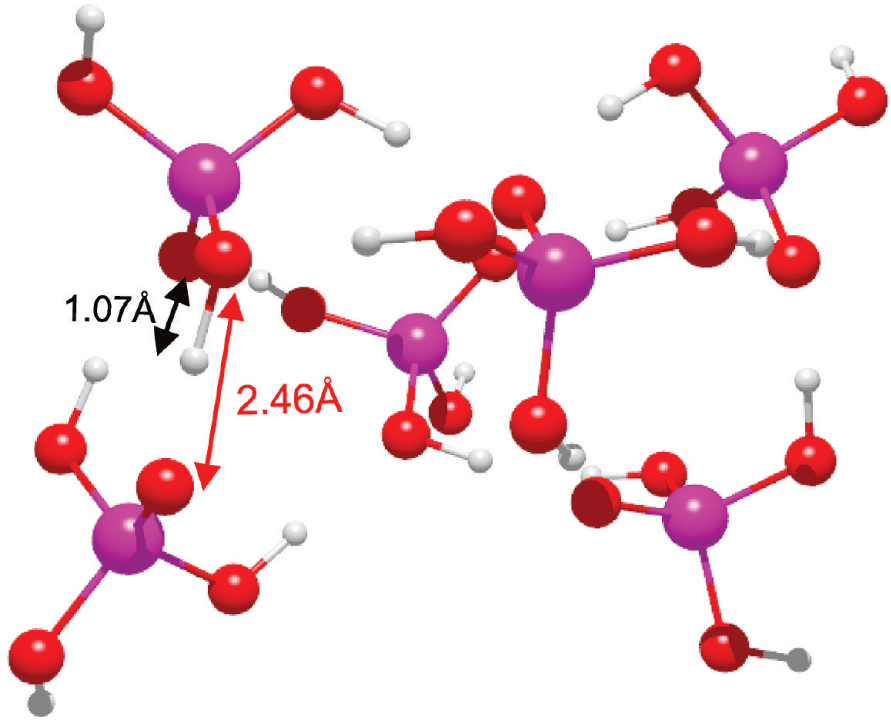

Figure 11. Fully optimized structures of $(H_3PO_4)_6$ determined at the B3LYP/6-311G** level.

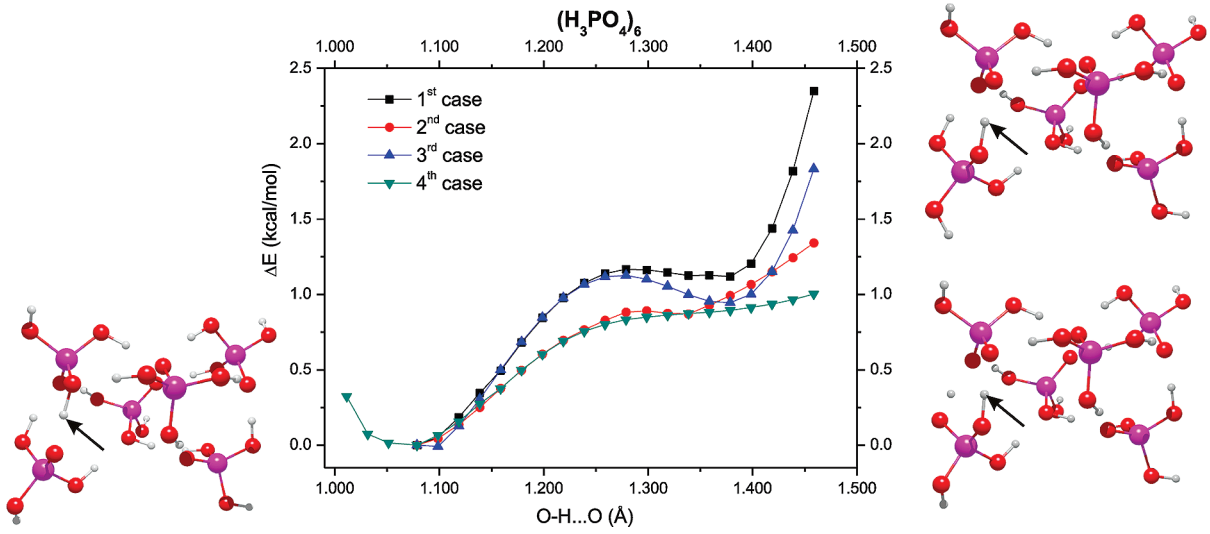

Figure 12. First case, constraint of the O···O distance of the hydrogen bond where the proton is transferred and the O−H bond length of the neighboring hydrogen bond; second case, constraint on the O−H bond length only; third case, constraint of the O···O distance of the hydrogen bond where the proton is transferred only; and fourth case, no constraints. The different configurations shown correspond to the fully optimized dimer (left), the structure following proton transfer under the first constraint (top right), and the structure resulting from proton transfer without any constraint, the fourth case (bottom right).

13a). Moreover, the charges resulting from transfer of the proton are also quite delocalized over the system; the sum of atomic partial charges on the conjugate acid is −0.568, with the rest being distributed over adjacent H_3PO_4 molecules and +0.664 on the conjugate base. The dramatic decrease in all barriers in $(H_3PO_4)_6$ and the endothermicities provides some evidence concerning the importance of system size on the intermolecular proton-transfer process and the long-range transport of protons in phosphoric acid.

IV. Conclusions

We have undertaken an investigation into the energetics of proton transfer in phosphoric acid clusters consisting of two to

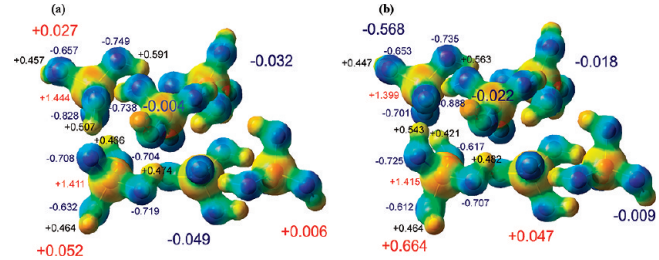

Figure 13. Partial atomic charges and electrostatic isosurface for the $(H_3PO_4)_6$ (a) before and (b) following proton transfer under the constraint of back transfer of the second proton (i.e., first case in Figure 12).

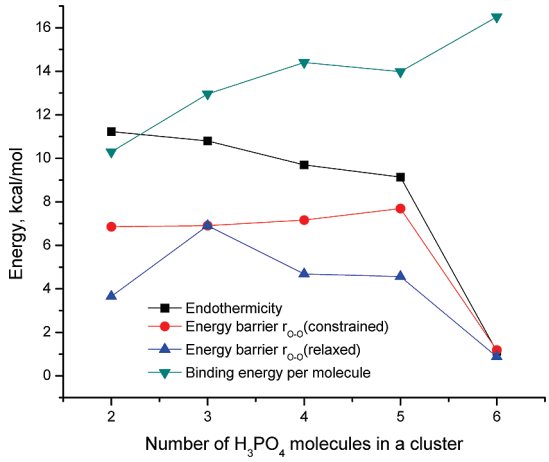

Figure 14. Energetic parameters as a function of cluster size; (a) endothermicity, (b) barrier for double proton transfer with the constraint of only the O−O bond length, (c) barrier for double proton transfer with the relaxed O−O bond length, and (d) the binding energy per H_3PO_4 molecule. (a), (b), and (c) were evaluated at the B3LYP/6-31G** level, and (d) was evaluated at the B3LYP/6-311G** level correction for both ZPE and BSSE.

six molecules. A number of initial configurations for each of the clusters were constructed in order to locate the global minimum-energy configuration. All structures were proved to be energy minima by frequency analysis. Binding energies per H_3PO_4 were computed and corrected for ZPE and BSSE and showed an increasing trend up to hexameric cluster, with only the pentamer representing a slight deviation. This observation may be attributed to the increase in the average number of hydrogen bonds per molecule and the interaction energies approaching those in the condensed phase. However, a cluster of six molecules is probably too small to observe saturation in those values, and investigation of larger and/or extended systems is necessary. Partial atomic charges determined for each molecule of the cluster prior and following proton transfer also reveal an increase in charge delocalization, which appears to facilitate the proton transfer with a lower energy barrier. The energetics are collected together in Figure 14 and clearly show an almost systematic decrease in the endothermicity with an increase in the number of molecules comprising the cluster. Interestingly, only the largest complex in our study demonstrates an abrupt decrease in the energy penalty accompanying the proton transfer. This effect may be due to the variation in the hydrogen bond length; however, this variation is more of a random fashion than showing a systematical extension or contraction according to the number of molecules in the cluster. Hence, there is obviously some indication of a decreasing energetic cost for the proton transfer and charge separation upon increase in the system's size, with the largest cluster representing the most extreme case in our study. Relaxation of the surrounding atoms has a systematic effect on the proton-transfer energetics. The change in the constraint on a neighboring O−H bond during calculations either forces or prevents the charge separation, thus completely changing the energetics of the proton-transfer process. The relaxed bond allows a neighboring proton to hop back; thus, double proton migration takes place, and the structure, in principle, transforms itself into the starting structure, with the profile of the energy barrier resembling a symmetric double well potential. The variation of activation barriers for the third and fourth cases versus cluster size is also shown in Figure 14. There is no uniform variation in these quantities; however, the largest system of six molecules shows a rapid "softening" of both barriers, which suggests a "critical cluster size" for the system. However, it was observed that several of the stable clusters readily rearranged into other configurations that were occasionally lower in energy upon a slight charge displacement during the transfer of a proton. These observations indicate significant freedom in configuration space existing in these systems comprised of only a relatively small number of molecules and that the local minima are closely related. This suggests that proton transport in neat phosphoric acid may be facilitated by these rearrangements, which respectively lower the activation barriers and endothermicities for charge separation.

Acknowledgment. L.V. gratefully acknowledges the financial support from Deutscher Akademischer Austausch Dienst (DAAD) and Max-Planck-Institut für Festkörperforschung. All calculations were performed on Itanium 2 clusters located at the University of Alabama, Huntsville, and the University of Tennessee, Knoxville.

References and Notes

(1) DeCoursey, T. E. *Physiol. Rev.* **2003**, *83*, 475.
(2) Elliott, J. A.; Paddison, S. J. *Phys. Chem. Chem. Phys.* **2007**, *9*, 2602.
(3) Kreuer, K. D. *J. Membr. Sci.* **2001**, *185*, 29.
(4) Agmon, N. *Chem. Phys. Lett.* **1995**, *244*, 456.
(5) Savadogo, O. *J. New Mater. Electrochem. Syst.* **1998**, *1*, 47.
(6) Savadogo, O. *J. Power Sources* **2004**, *127*, 135.
(7) Kreuer, K. D. *Chem. Mater.* **1996**, *8*, 610.
(8) Markovitch, O.; Chen, H.; Izvekov, S.; Paesani, F.; Voth, G. A.; Agmon, N. *J. Phys. Chem. B* **2008**, *112*, 9456.
(9) Dominik, M. *ChemPhysChem* **2006**, *7*, 1848.
(10) Paddison, S. J.; Elliott, J. A. *Phys. Chem. Chem. Phys.* **2006**, *8*, 2193.
(11) Paddison, S. J. Proton Conduction in PEMs: Complexity, Cooperativity and Connectivity. In *Device and Materials Modeling in PEM Fuel Cells*; Paddison, S. J., Promislow, K. S., Eds.; Springer-Verlag: Berlin,Germany, 2009; Vol. 113, pp 385.
(12) Kreuer, K. D.; Paddison, S. J.; Spohr, E.; Schuster, M. *Chem. Rev.* **2004**, *104*, 4637.
(13) von Grotthuss, C. J. D. *Ann. Chim.* **1806**, *58*, 54.
(14) Tuckerman, M.; Laasonen, K.; Sprik, M.; Parrinello, M. *J. Phys. Chem.* **1995**, *99*, 5749.
(15) Tuckerman, M.; Laasonen, K.; Sprik, M.; Parrinello, M. *J. Chem. Phys.* **1995**, *103*, 150.
(16) Car, R.; Parrinello, M. *Phys. Rev. Lett.* **1985**, *55*, 2471.
(17) Eigen, M.; Demaeyer, L. *Proc. R. Soc. London, Ser. A* **1958**, *247*, 505.
(18) Eigen, M. *Angew. Chem., Int. Ed. Engl.* **1963**, *75*, 489.
(19) Zundel, G.; Metzger, H. *Z. Naturforsch. A: Phys. Sci.* **1967**, *22*, 1412.
(20) Schmitt, U. W.; Voth, G. A. *J. Chem. Phys.* **1999**, *111*, 9361.
(21) Tuckerman, M. E.; Marx, D.; Klein, M. L.; Parrinello, M. *Science* **1997**, *275*, 817.
(22) Marx, D.; Tuckerman, M. E.; Hutter, J.; Parrinello, M. *Nature* **1999**, *397*, 601.
(23) Marx, D.; Tuckerman, M. E.; Parrinello, M. *J. Phys.: Condens. Matter* **2000**, *12*, A153.
(24) Lobaugh, J.; Voth, G. A. *J. Chem. Phys.* **1996**, *104*, 2056.
(25) Sammes, N.; Bove, R.; Stahl, K. *Curr. Opin. Solid State Mater. Sci.* **2004**, *8*, 372.
(26) Wainwright, J. S.; Wang, J. T.; Savinell, R. F.; Litt, M. H. *J. Electrochem. Soc.* **1995**, *142*, L121.
(27) Ma, Y. L.; Wainright, J. S.; Litt, M. H.; Savinell, R. F. *J. Electrochem. Soc.* **2004**, *151*, A8.
(28) He, R.; Li, Q.; Xiao, G.; Bjerrum, N. J. *J. Membr. Sci.* **2003**, *226*, 169.
(29) Steininger, H.; Schuster, M.; Kreuer, K. D.; Kaltbeitzel, A.; Bingol, B.; Meyer, W. H.; Schauff, S.; Brunklaus, G.; Maier, J.; Spiess, H. W. *Phys. Chem. Chem. Phys.* **2007**, *9*, 1764.
(30) Munson, R. A. *J. Phys. Chem.* **1964**, *68*, 3374.
(31) Dippel, T.; Kreuer, K. D.; Lassègues, J. C.; Rodriguez, D. *Solid State Ionics* **1993**, *61*, 41.
(32) Aihara, Y.; Sonai, A.; Hattori, M.; Hayamizu, K. *J. Phys. Chem. B* **2006**, *110*, 24999.
(33) Greenwood, N. N.; Thompson, A. *Proc. Chem. Soc., London* **1958**, 352.
(34) Greenwood, N. N.; Thompson, A. *J. Chem. Soc.* **1959**, 3485.

(35) Spieser, S. A. H.; Leeflang, B. R.; Kroon-Batenburg, L. M. J.; Kroon, J. *J. Phys. Chem. A* **2000**, *104*, 7333.
(36) Tsuchida, E. *J. Phys. Soc. Jpn.* **2006**, *75*, 054801.
(37) Paddison, S. J.; Kreuer, K. D.; Maier, J. *Phys. Chem. Chem. Phys.* **2006**, *8*, 4530.
(38) Frisch, M. J.; Trucks, G. W.; Schlegel, H. B.; Scuseria, G. E.; Robb, M. A.; Cheeseman, J. R.; Montgomery, J., J. A. ; Vreven, T.; Kudin, K. N.; Burant, J. C.; Millam, J. M.; Iyengar, S. S.; Tomasi, J.; Barone, V.; Mennucci, B.; Cossi, M.; Scalmani, G.; Rega, N.; Petersson, G. A.; Nakatsuji, H.; Hada, M.; Ehara, M.; Toyota, K.; Fukuda, R.; Hasegawa, J.; Ishida, M.; Nakajima, T.; Honda, Y.; Kitao, O.; Nakai, H.; Klene, M.; Li, X.; Knox, J. E.; Hratchian, H. P.; Cross, J. B.; Bakken, V.; Adamo, C.; Jaramillo, J.; Gomperts, R.; Stratmann, R. E.; Yazyev, O.; Austin, A. J.; Cammi, R.; Pomelli, C.; Ochterski, J. W.; Ayala, P. Y.; Morokuma, K.; Voth, G. A.; Salvador, P.; Dannenberg, J. J.; Zakrzewski, V. G.; Dapprich, S.; Daniels, A. D.; Strain, M. C.; Farkas, O.; Malick, D. K.; Rabuck, A. D.; Raghavachari, K.; Foresman, J. B.; Ortiz, J. V.; Cui, Q.; Baboul, A. G.; Clifford, S.; Cioslowski, J.; Stefanov, B. B.; Liu, G.; Liashenko, A.; Piskorz, P.; Komaromi, I.; Martin, R. L.; Fox, D. J.; Keith, T.; Al-Laham, M. A.; Peng, C. Y.; Nanayakkara, A.; Challacombe, M.; Gill, P. M. W.; Johnson, B.; Chen, W.; Wong, M. W.; Gonzalez, C.; and Pople, J. A. *Gaussian 03* revision C.02; Gaussian Inc.: Wallingford, CT, 2004.
(39) Schlegel, B. H. *J. Comput. Chem.* **1982**, *3*, 214.
(40) Hariharan, P. C.; Pople, J. A. *Theor. Chim. Acta* **1973**, *28*, 213.
(41) Becke, A. D. *J. Chem. Phys.* **1993**, *98*, 1372.
(42) Becke, A. D. *J. Chem. Phys.* **1993**, *98*, 5648.
(43) Lee, C.; Yang, W.; Parr, R. G. *Phys. Rev. B* **1988**, *37*, 785.
(44) Boys, S. F.; Bernardi, F. *Mol. Phys.* **1970**, *19*, 553.
(45) Kobko, N.; Dannenberg, J. J. *J. Phys. Chem. A* **2001**, *105*, 1944.
(46) Breneman, C. M.; Wiberg, K. B. *J. Comput. Chem.* **1990**, *11*, 361.
(47) Blessing, R. H. *Acta Crystallogr.* **1988**, *B44*, 334.
(48) Blessing, R. H. *Acta Crystallogr.* **1989**, *B45*, 200.

JP903005R